Argemone Mexicana plant, Papaveraceae family, contains excellent medicinal properties. Accordingly, *Argemone Mexicana* is used in the formation of several Ayurvedic drugs. However, this plant shows toxicity that restricts its wide application without proper control. An extensive study has been done on Argemone Mexicana by Dash et al [2011], which states that aqueous extract of Argemone Mexicana leaves does not show toxicity. The aqueous extract of the plant's leaves contain proteins, amino acids, tannins, phenolic compounds, saponins and flavonoids as well as non-alkaloids organic compounds (the toxicity of the plant belongs to alkaloids) like fused benzene rings, hetero N atom rings, -OCH_3 and -OH groups. Hence, we have chosen aqueous extract of Argemone Mexicana plant's leaves for corrosion inhibition study. The results of the investigation are discussed under following sections.

3.1 Characterization of Argemone Mexicana Leaf Extract

FTIR Spectroscopy: Figure 8 illustrates FT-IR spectrum of the aqueous *Argemone Mexicana* leaves extract (AMLE), which indicates presence of various functional groups. A Broad band at 3294 cm^{-1} can be assigned to N-H or O-H stretching vibration. An absorption peak at 2114 cm^{-1} is found due to N=C=S stretching vibration. A Strong peak obtained at 1636 cm^{-1} can be correlated to C=C, or C=N stretching, or N-H bending frequency. An Absorption peak at 1402 cm^{-1} can be assigned to C-H bending in $–CH_3$ or O-H bending vibration. The Peaks obtained in the range of 1000 to 1200 cm^{-1} (1030, 1080 and 1124 cm^{-1}) can be related to C-N and C-O stretching vibration. Few weak peaks can also be noticed at 1430 cm^{-1}, 1450 cm^{-1} and 1600 cm^{-1}, which correspond to C=C stretching frequencies of aromatic rings. Thus, as a result of the investigation, it can be concluded that AMLE contain nitrogen and oxygen (N-H,N=C=S,C=N,C-N,O-H,C=O,C-

O) in various functional groups along with aromatic rings , which confirms the presence of bioactive compounds in the leaf extract.

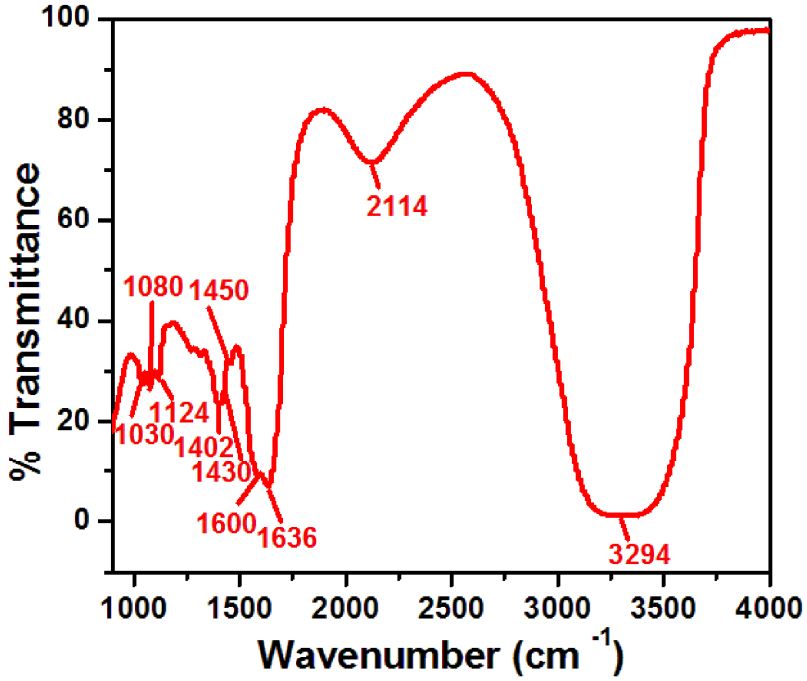

Figure 3.1 FT-IR spectrum of aqueous leaf extract of *Argemone Mexicana*

UV-visible Spectroscopy: The molecular electronic transitions of inhibitors were investigated using this technique in the range of 200-800 nm. The liquid samples of the extracts were put in a quartz cuvette and analyzed by UV-Vis spectrophotometer. Figure 9 shows UV-Vis spectrum of aqueous *Argemone Mexicana* leaf extract. A broad peak at 276 nm was observed in the spectrum, which was due to presence of aromatic rings in the extract. Along with a peak at 276 nm, few small bands could be clearly seen in the obtained spectrum, which could be related to presence of aromatic compounds in the plant extract [*C. Kamal* et al., 2012].

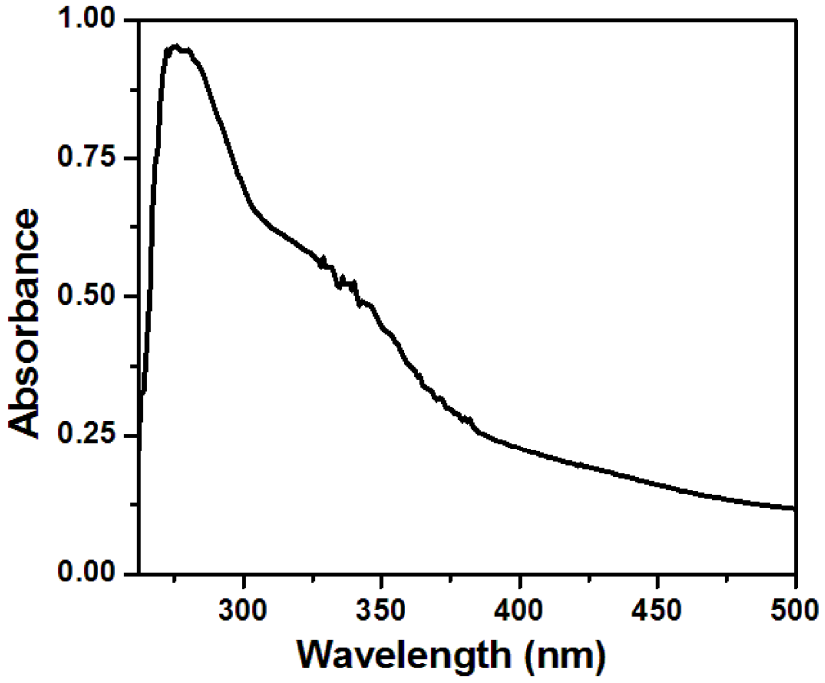

Figure 3.2 UV-Vis Spectrum of Argemone Mexicana aqueous leaf extract

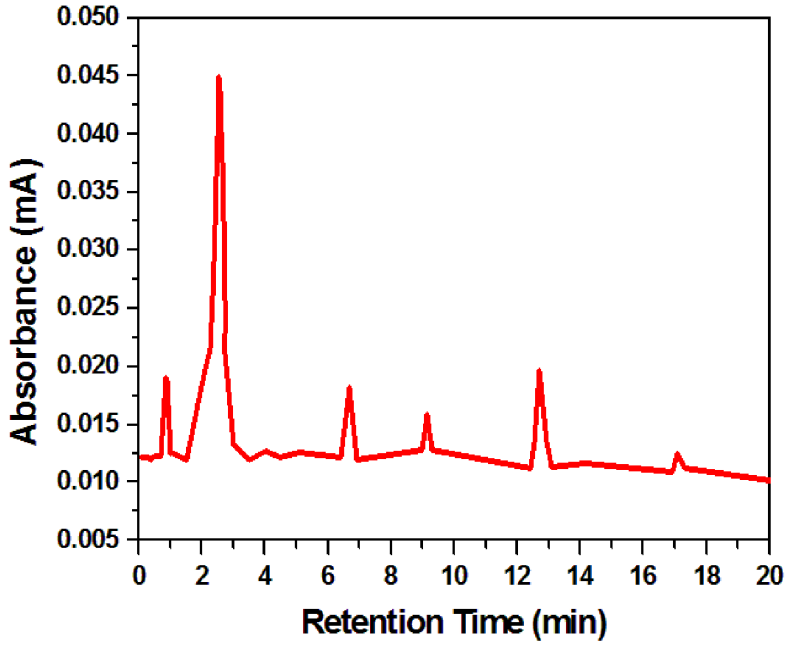

Figure 3.3 HPLC Chromatograph of Argemone Mexicana Leaves extract

High Pressure Liquid Chromatography: Argemone Mexicana is a well known plant since ancient age. A number of works have been done on the plant's properties and its phytochemical constituents. Yet, we have done chromatographic analysis of the extract.

Figure 10 illustrates chromatogram of Argemone Mexicana leaf extract. In the chromatograph, several peaks were appeared corresponding to different chemical compounds of the extract. We did not go for identification of each compound as it would be a tedious and difficult job (the constituents are well known); however, we tried to show the complex chemical nature of the aqueous *Argemone Mexicana* extract.

3.2 Weight Loss Measurements

Corrosion behavior of Mild steel in HCl and H_2SO_4 solutions was investigated by weight loss measurements technique. Results indicated that mild steel samples corroded at a very fast rate in 1M HCl and 0.5 M H_2SO_4, while addition of different concentration of AMLE caused significant reduction in corrosion rate. In both acid media, inhibition efficiency was found increasing with increase in the extract concentration. Through careful investigation of Table 1 (1 M HCl), it was evident that corrosion rates retarded with the inhibitor concentration while inhibition efficiency increased. At 500 mgL^{-1} amount of AMLE, saturation occurred and nearly 93% corrosion inhibition was achieved. After this concentration of the extract, any appreciable change in inhibition efficiency was not observed.

Figure 11 summarizes results of the weight loss method for mild steel corrosion in sulfuric acid. Through carful inspection of the results, it was observed that the rate of mild steel corrosion in H_2SO_4 was very high (C_r=37.60 mmpy); however, a significant reduction in the corrosion rate (5.26 mmpy) was observed for 600 mg L^{-1} AMLE concentration. This indicated enhanced corrosion resistance of mild steel in presence of inhibitor. The fact mentioned above could be clearly observed through changes in the

value of inhibition efficiency, i.e., inhibition increased with the concentration and a maximum efficiency of 86 % was obtained at 600 mg L^{-1} amount of the extract.

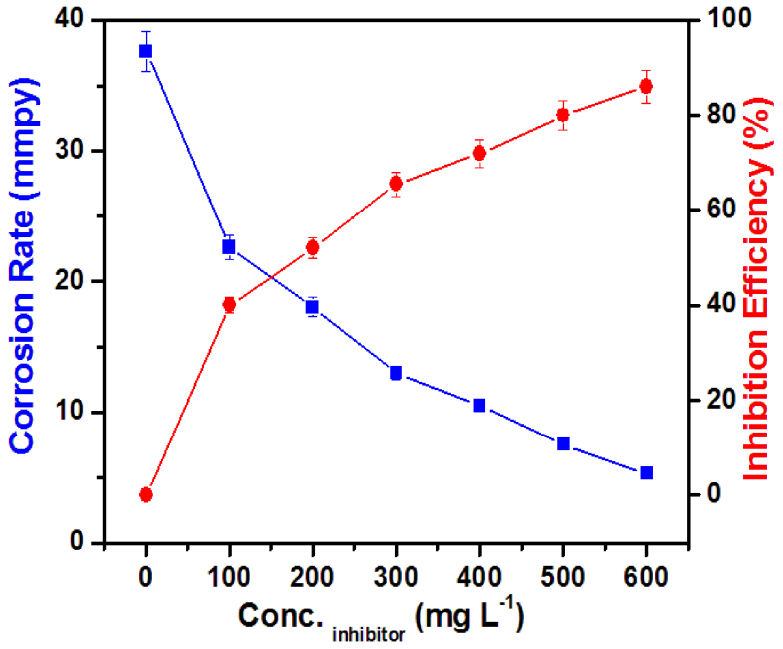

Figure 3.4 Corrosion rate and inhibition efficiency at various concentrations of AMLE in 0.5 M sulfuric acid at 27±1° C for 5h

Table 3.1 Corrosion parameters for mild steel in 1M HCl in absence and presence of different concentrations of AMLE obtained by weight loss measurements at 27±1°C for 5 hrs

Conc. of Inhibitor (mgL^{-1})	Weight loss ($mg\ cm^{-2}$)	Inhibition Efficiency $\mu_{WL}(\%)$	Corrosion rate (*mmpy*)	Surface Coverage (θ)	C_{inh} / θ (mgL^{-1})
Blank	15.40	-	34.3	-	-
50	11.97	22.27	26.7	0.2227	224.5
100	8.63	43.96	19.2	0.4396	227.5
200	3.65	76.30	8.1	0.7630	262.2
300	2.05	86.69	4.6	0.8669	346.1
400	1.88	87.79	4.2	0.8779	455.6
500	**1.15**	**92.53**	**2.6**	**0.9253**	**540.4**
600	1.15	92.53	2.6	0.9253	648.4

On the basis of the results obtained, it could be concluded that Argemone Mexicana leaf extract efficiently retarded mild steel corrosion in both acid media; however, performance of the extract was more effective in HCl than in H_2SO_4.

3.2.1 Adsorption Analysis

Adsorption of an organic moiety depends on many factors, such as, the charge and the nature of metal surface, adsorption of solvent and other ionic species and the electrochemical potential at solution interface. The corrosion inhibition efficiency of a corrosion inhibitor is greatly related with the ability of it to cover the metal surface. Hence, it becomes necessary to investigate metal inhibitor interaction through adsorption isotherms. The most frequently used adsorption isotherms are Langmuir, Temkin, Frumkin, Freundluich isotherms. The Langmuir isotherm equation has been already mentioned in introduction part (Eq.15).

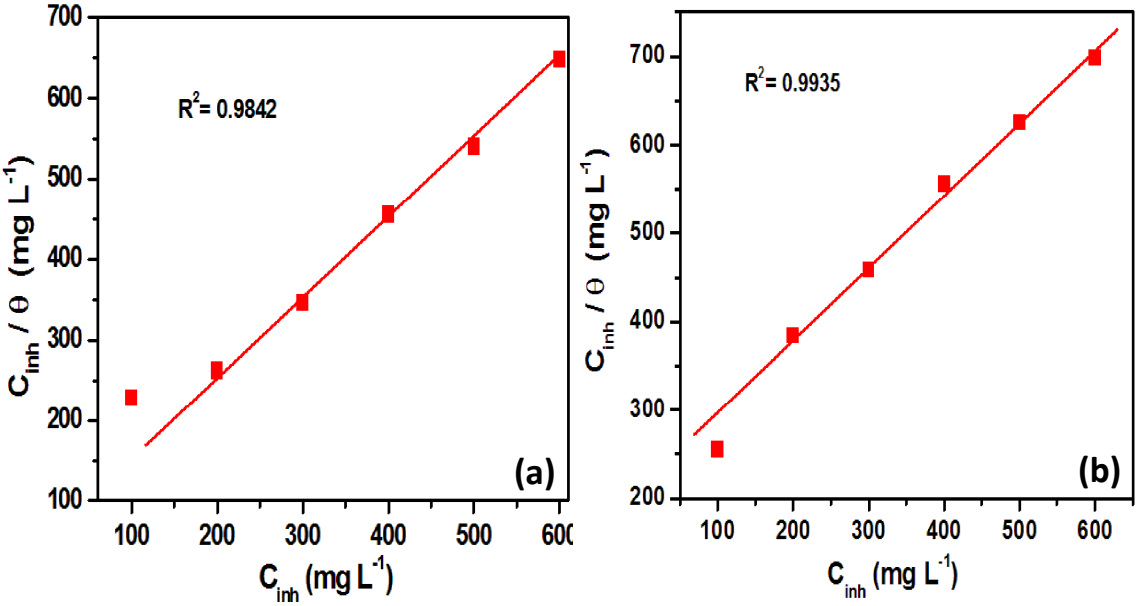

Figure 3.5 Langmuir isotherm fitting for mild steel in (a) 1 M HCl and (b) H_2SO_4 solutions

Figure 12 demonstrates Langmuir isotherm fitting for mild steel in acid solutions. The regression coefficient R^2 was found almost unity (HCl-0.98424, H_2SO_4-0.9935), which favored our approach towards adsorption isotherm. Figure 13 illustrates UV-Vis spectra of pure extract and washing of the solutions containing adsorbed extract molecules on mild steel surface in HCl and H_2SO_4 media. It is evident from the graph that the spectra showed similar pattern in either case, suggesting that almost all the organic compounds of the Argemone Mexicana extract were adsorbed on the metal surface. Hence, it could be stated that inhibition potential of the extract was closely related with the adsorption process.

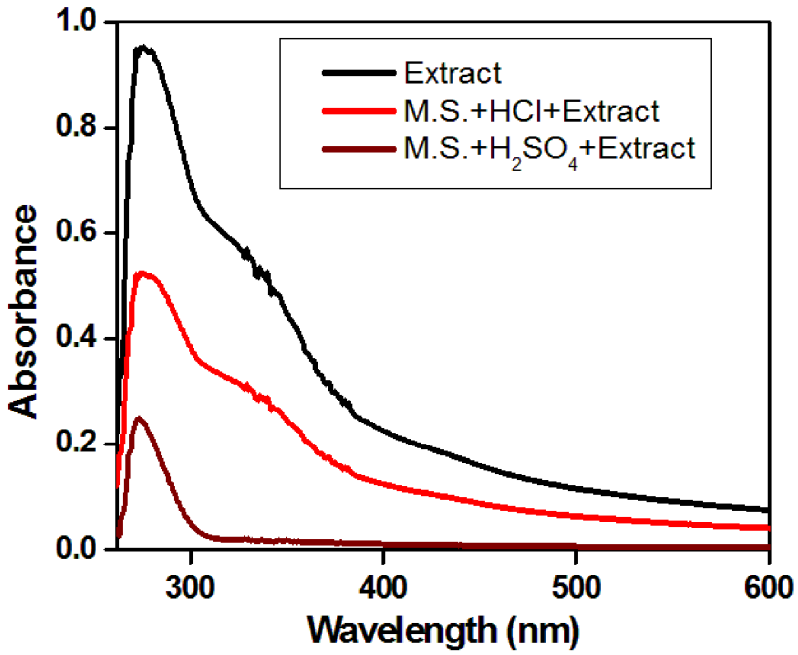

Figure 3.6 Showing UV-Vis spectra of pure extract and mild steel in HCl and H_2SO_4 in presence of maximum extract concentration

Further, the value of ΔG^0 was determined by equation 21 at room temperature. The ΔG^0 value in HCl was 24.10 kJ mol^{-1}, while it was 21.10 kJ mol^{-1} in H_2SO_4. This fact revealed that adsorption of inhibitor molecules over mild steel was almost physical adsorption ($\Delta G^0 \geq$ -20 kJ mol^{-1}, Physical adsorption) [*I.B. Obot* et al., 2011, Tebbji et al., 2007].

3.2.2 Effect of Immersion Time

The stability of the extract was checked by weight loss method for 120 hours at room temperature. It is evident from the Figure 14 that corrosion rates of mild steel in acid media sharply increased in first 60 hours, slowly increased during 60 to 84 hours and attained a saturated value in the rest of the time. On the other hand, corrosion rates of mild steel in acid media were significantly retarded in presence of the extract. However, a slight increase in rate of corrosion reactions was noticed with the immersion time, which showed degradation of the inhibitor molecules or desorption from metal surface [Bentiss et al., 2005; A.K. Singh 2012].

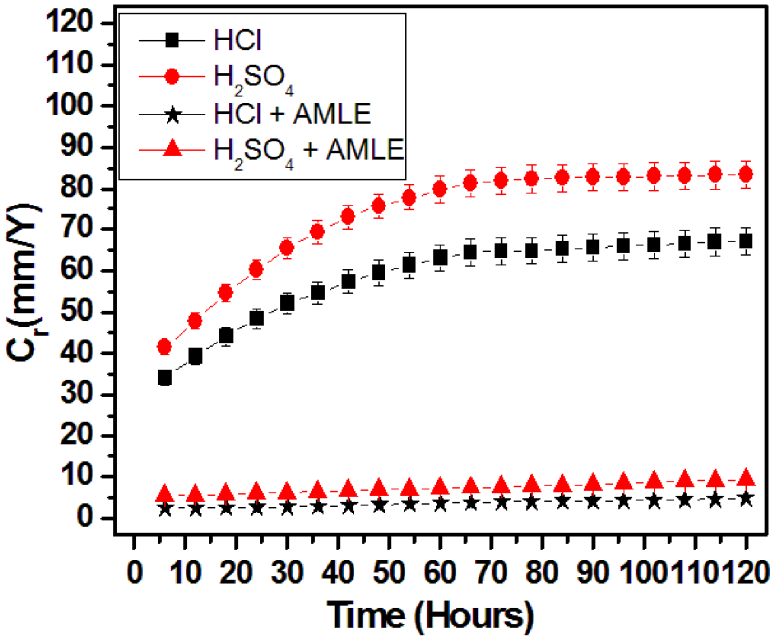

Figure 3.7 Showing effect of immersion time on inhibition potential of the AMLE

3.2.3 Effect of Acid Concentration

An important aspect of the corrosion inhibition study is to investigate inhibition efficiency variation as a function of acid concentration. Figure 15 summarizes the results obtained for inhibited mild steel in different concentration of acid solutions by weight

loss method. Through investigation of the results, it was revealed that corrosion rate of mild steel rapidly increased in HCl and H_2SO_4 alone. On the opposite side, mild steel corrosion was successfully inhibited by the extracts. However, inhibition efficiency decreased with the concentration of acid in both cases. The decrease in inhibition efficiency could be attributed to decreased rate of molecular adsorption, or faster degradation of the extract molecules with increase in acid concentration [Mathur and Vasudevan, 1982].

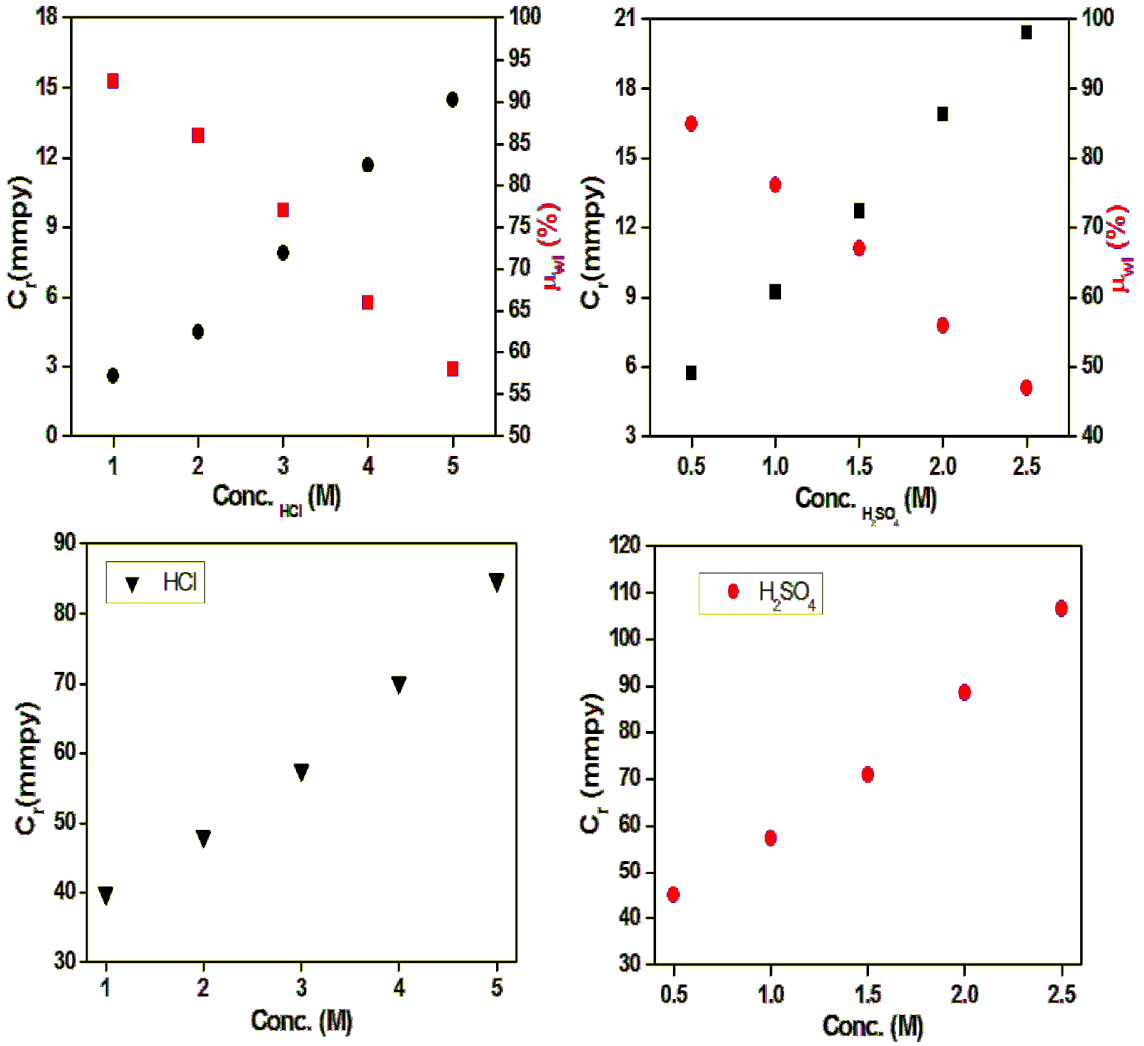

Figure 3.8 Corrosion rates and inhibition efficiencies obtained for mild steel in HCl and H_2SO_4 alone and in presence of the extracts (maximum concentration) by weight loss method at room temperature.

3.2.4 Effect of Temperature on Corrosion Parameters

The relation of activation energy, corrosion rate and temperature can be described by Arrhenius equation (Eq. 18). It is evident from the equation that corrosion rate increases exponentially with the temperature. Hence, to test corrosion inhibitor performance with the temperature becomes necessary.

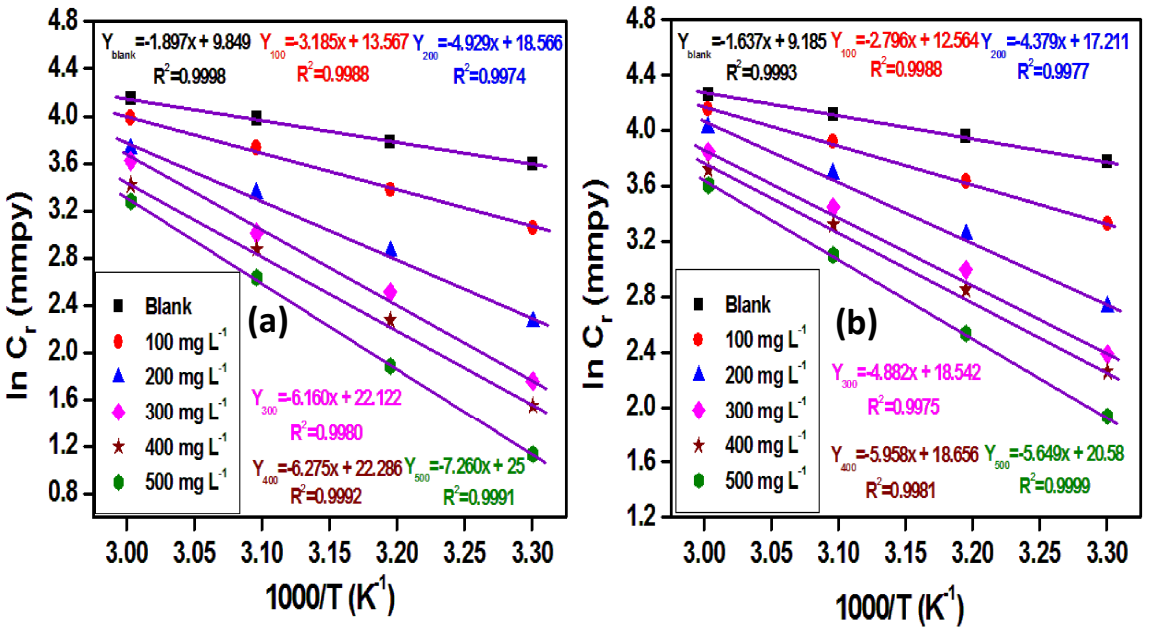

Figure 3.9 Arrhenius plot for mild steel in (a) 1 M HCl and (b) 0.5 M H_2SO_4 with different concentrations of AMLE

Effect of temperature on inhibition potential of AMLE was investigated in 1 M HCl and 0.5 M H_2SO_4 by weight loss method in the range of 30˚-60˚ C. Figure 16 illustrates that slope and intercept values of the curves increased with the inhibitor concentration in both acid media. This fact suggested that activation energy and Arrhenius coefficient value increased with the addition of Argemone Mexicana extract in HCl and H_2SO_4 solutions, which showed physical adsorption of the extract molecule over mild steel surface [Martinez and Stern, 2002; Sorkhabi et al., 2005]. However, greater values of activation energy were achieved in hydrochloric acid than sulfuric acid for a particular inhibitor

concentration. The similar information was obtained from the corrosion parameters calculated from the Arrhenius curves (Table 2). In the view of above mentioned facts, it could be stated that addition of inhibitor hoisted the limit of energy barrier for corrosive molecules. Accordingly, better corrosion inhibition was acknowledged with respect to blank acid solutions.

Table 3.2 Activation parameters for mild steel in 1 M HCl without and with different concentrations of AMLE

Solution	Conc. of Inhibitor (mg L^{-1})	A (mmpy)	Ea (kJ mol^{-1})	Δ H* (kJ mol^{-1})	ΔS* (J mol^{-1} K^{-1})	E_a- ΔH* (kJ mol^{-1})
HCl	Blank	18.92×10^3	15.77	13.12	-171.78	2.65
	100	7.78×10^5	26.48	23.84	-140.87	2.64
	200	1.15×10^8	40.97	38.33	-99.31	2.64
	300	4.04×10^9	51.21	48.57	-69.76	2.64
	400	4.76×10^9	52.17	49.53	-68.37	2.64
	500	7.18×10^{10}	60.35	57.71	-45.05	2.64
H_2SO_4	Blank	9.74×10^3	13.61	10.97	-177.25	2.64
	100	2.85×10^5	23.24	20.60	-149.23	2.64
	200	2.97×10^7	36.40	33.77	-110.50	2.63
	300	1.12×10^8	40.58	37.95	-99.36	2.63
	400	1.24×10^8	40.92	38.28	-98.82	2.64
	500	8.64×10^8	46.96	44.33	-82.55	2.63

The other activation parameters, such as, change in enthalpy (ΔH^*) of activation and entropy (ΔS^*) of activation, were determined by Transition state equation (Eq. 19). From careful investigation of the parameters listed in Table 2, it was revealed that the differences between ΔH^* values of uninhibited and inhibited mild steel increased with the extract concentration. Also, ΔH^* were having positive values at each concentration of inhibitor. In the view of above mentioned facts it could be concluded that AMLE increased the value of required energy for mild steel corrosion, indicating that metal

dissolution in presence of the extract was not easy for corroding molecules (Figure 17) [Mu et al., 2004; Lashgari and Malek, 2010]. However, greater values of ΔH^* was acknowledged in HCl than values obtained in H_2SO_4 indicating that the extract was more efficient in hydrochloric acid. Further, it could be noticed from Table 2 that there was a relation between ΔH^* and E_a, which was found in accordance with the following equation-

$$\Delta H^* = E_a - RT \qquad (22)$$

We got almost constant value of E_a- ΔH^* in both acid media, which verified the experimental results of thermodynamic experiments.

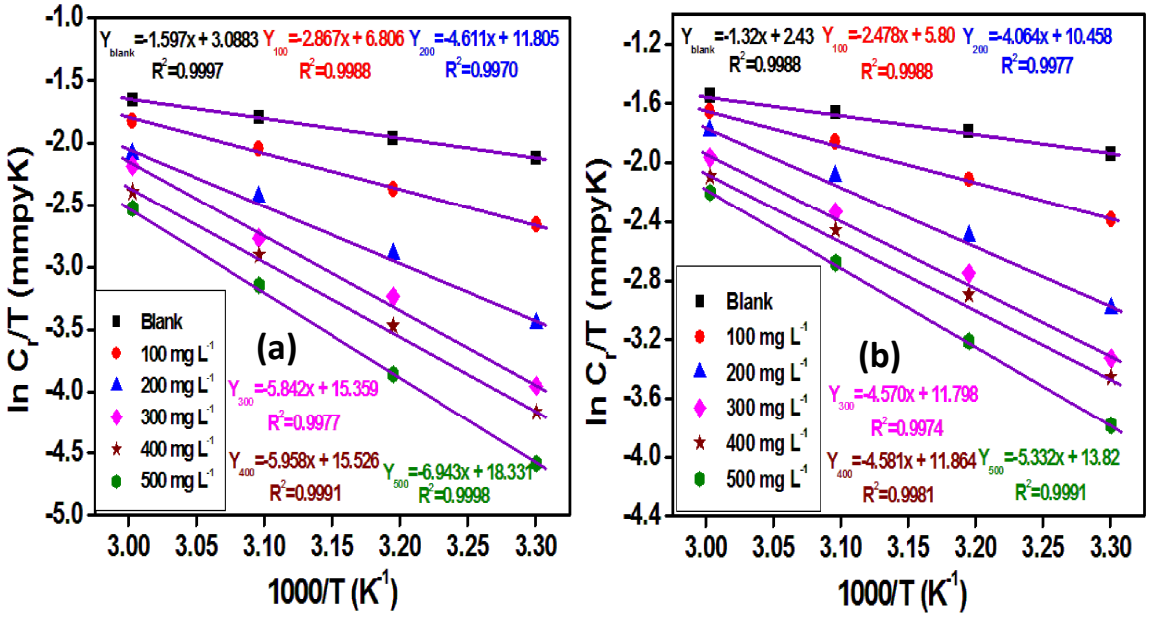

Figure 3.10 Transition state plot for mild steel in (a) 1 M HCl and (b) 0.5 M H_2SO_4 with different concentrations of AMLE

Another important parameter of temperature dependent corrosion study is entropy of activation, which reflects randomness of the molecular adsorption. Through analysis of the ΔS^* values, it was observed that randomness of the system increased with the

increase in inhibitor concentration. The reason of this incident could be given as conversion of reactants into activated complex, which might resulted from adsorption of the extract molecules on mild steel [Sahin et al., 2002]. Basically, adsorption of the organic molecules on metals in aqueous solutions is regarded as quasi-substitution reactions between water molecules and inhibitor molecules. Accordingly, it could be stated that the extract molecules displaced water molecules from the metal surface causing increase in entropy of activation, which occurred due to increase in entropy of the solvent [Ateya et al., 1984]. However, more positive values of ΔS^* was achieved in HCl solution than H_2SO_4 solution indicating that the inhibitor retarded the temperature effect more effectively in hydrochloric acid in comparison to sulfuric acid.

3.3 Tafel Polarization Curves

The polarization behavior of mild steel was investigated in both acid solutions in presence and absence of the extract. Figure 18 and 19 illustrate the effect of AMLE on mild steel corrosion in 1M HCl and 0.5 M H_2SO_4, respectively. It was observed from the polarization curves that the cathodic and anodic reactions (both cases) were diminished with the addition of the extract. Accordingly, it could be concluded that AMLE decreased the rate of anodic dissolution reactions as well as retarded the hydrogen evolution reactions on the cathodic sites. The electrochemical kinetics parameters, i.e., corrosion potential (E_{corr}), corrosion current density (I_{corr}), anodic and cathodic Tafel slopes (b_a and b_c), were listed in Table 3 and 4.

It is evident from Table 3 that magnitude of b_c significantly changed with increase in inhibitor concentration, indicating effect of the extract on the kinetics of the hydrogen

evolution reaction. The shift in the value of anodic Tafel slope b_a clearly showed changes occurred at anodic sites, which might be related to the chloride ion /or inhibitor molecules adsorption on the metal surface. Further investigation of the results revealed that the corrosion current density (I_{corr}) decreased by increasing the inhibitor concentration, hence corrosion rate of mild steel retarded. The maximum difference of free corrosion potential with respect blank solution was acknowledged as 49 mV. According to Ferreira et al. [2004] and Li et al. [2008], if the displacement in corrosion potential is more than 85 mV with respect to the corrosion potential of blank solution, the inhibitor can be consider as a cathodic or anodic type. This indicated that the studied inhibitor was a mixed type inhibitor.

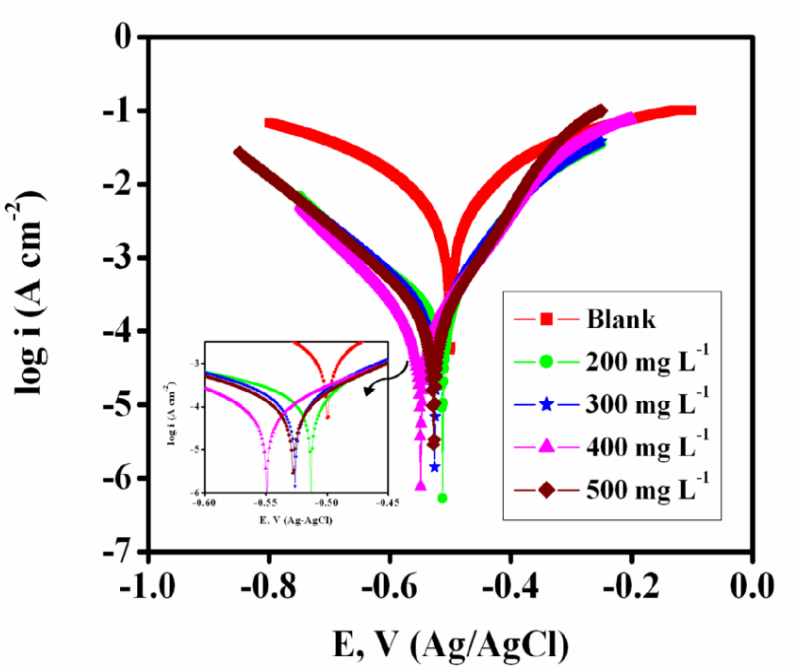

Figure 3.11 Tafel plot of mild steel in 1M HCl with different concentrations of AMLE in 1M HCl solution

Table 3.3 Potentiodynamic polarization parameters for mild steel without and with different concentrations of AM extract in 1M HCl solution.

Conc. of inhibitor (mgL^{-1})	$-E_{corr}$ (mV vs Ag/AgCl)	I_{corr} ($\mu A\ cm^{-2}$)	b_a ($mV\ dec^{-1}$)	b_c ($mV\ dec^{-1}$)	μ_p (%)
Blank	500	1220	60	114	-
200	513	264	97	160	78.4
300	526	213	103	171	82.5
400	549	140	112.2	182	88.5
500	**528**	**108**	**131.4**	**174**	**91.2**

.

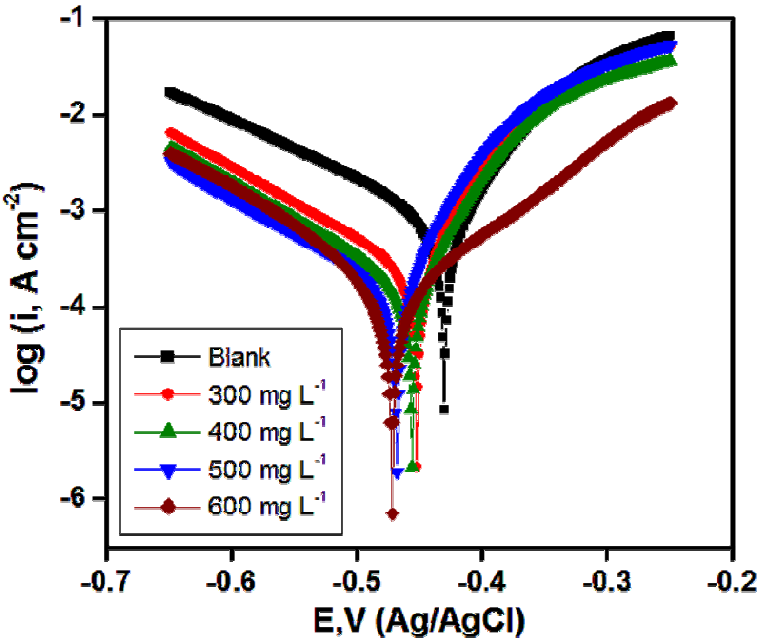

Figure 3.12 Polarization curve plot for mild steel in 0.5 M sulfuric acid with different concentrations of *AMLE*

In case of H_2SO_4 exposure, the shift in the values of cathodic and anodic slope, i.e., b_c and b_a, was not sharp meaning that the extract molecules retarded corrosion reaction by working in a mode of mixed type inhibition (Table 4). The maximum displacement in E_{corr} value was observed as 42 mV, suggesting that the AMLE was a mixed type inhibitor

Table 3.4 Parameters obtained from polarization curves at different concentration of inhibitor for 0.5 M sulfuric acid.

Conc. (mg L^{-1})	-Ecorr (mV , Ag/AgCl)	I corr (µA cm^{-2})	b_a (mV dec^{-1})	b_c (mV dec^{-1})	μ_p %
Blank	430	1138	93	62	-
300	452	450	90	76	60
400	456	304	94	75	73
500	468	250	102	73	78
600	**472**	**145**	**96**	**79**	**87**

As a conclusion of the Tafel polarization test it could be stated that AMLE suppressed both anodic and cathodic partial reactions and significantly decreased I_{corr} values. Thus, mild steel corrosion in HCl and H_2SO_4 was inhibited by using Argemone Mexicana aqueous leaf extract.

3.4 Electrochemical Impedance Spectroscopy

Corrosion behavior of mild steel in 1.0 M hydrochloric acid and 0.5 M sulfuric acid solutions was studied in absence and presence of *Argemone Mexicana* extract by electrochemical impedance spectroscopy technique. Figure 20 and 21 illustrated results of impedance experiments. A single semicircle was observed at high frequency in both the cases, indicating that corrosion of mild steel was governed by charge transfer reactions. Additionally, it could be seen that the diameter of the circle was increasing with the concentration in either cases. This fact revealed that charge transfer resistance value increased with the amount of the extracts. Figure 20 and 21 clearly showed that the impedance spectra were not perfect semicircle. In more precise word, it was depressed

with centre under real axis and resembled as depressed capacitive loops. Such cases often correspond to surface heterogeneity, which may be the result of surface roughness, dislocations and distribution of the active sites, or adsorption of the inhibitor molecules [Fawcett et al. 1992; Solomon et al., 2010]. An equivalent electrochemical circuit (Inset-Figure 20) was used to simulate the results of EIS. In this circuit R_s is solution resistance, R_t is charge transfer resistance and CPE is a constant phase element. The impedance value of the CPE can be described as follows:

$$Z_{CPE} = Y^{-1}(j\omega)^{-n} \quad (23)$$

where *Y i*s the magnitude of the CPE, ω is the angular frequency and *n* is a valuable physical parameter showing phase angle difference. Actually, n is related with the microscopic fluctuations occurring at the metal-acid interface. If we analyze the equation 22, it is evident that Z_{CPE} represents a resistance with $R=Y^{-1}$ (for n=0); an inductance with $L=Y^{1}$ (for n=-1) and an ideal capacitor with $C=Y$ (n=1). In iron/acid interface systems, ideal capacitor behavior (n=1) is not observed because of the surface roughness or uneven current distributions on the electrode surface, causing frequency dispersion [Rammelt et al., 1987; Pang et al., 1990].

The electrochemical parameters of corrosion (R_s, R_t, Y_o, C_{dl} and n) were calculated by fitting the EIS data using equivalent circuit shown in inset of Figure 21. The values of double layer capacitance C_{dl} (listed in Table 5 and 6) were derived from CPE parameters by the following equation [Umoren et al., 2011, Barouni et al., 2010]-

$$C_{dl} = (Y_o . R_t^{1-n})^{1/n} \quad (24)$$

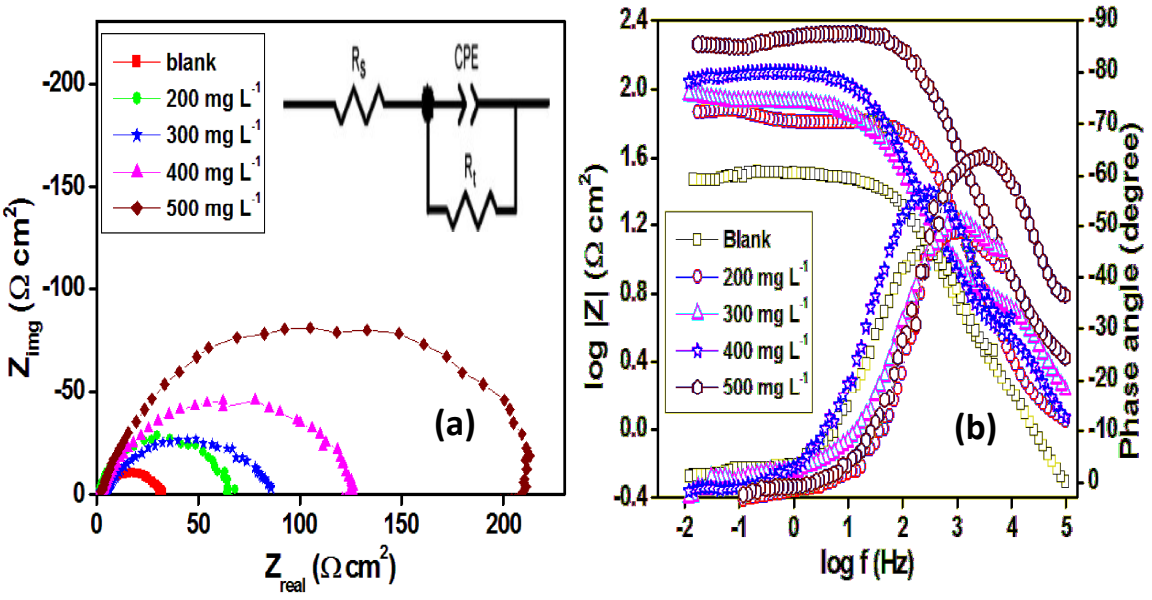

Figure 3.13 Showing (a) Nyquist plot and (b) bode plot for mild steel in 1M HCl in absence and presence of AMLE.

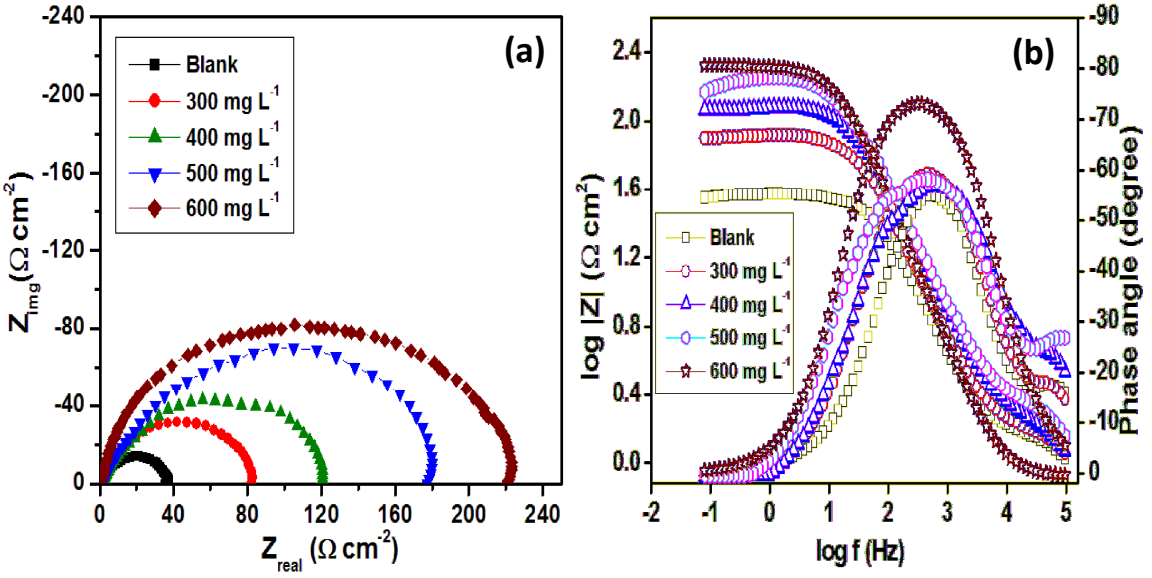

Figure 3.14 Showing (a) Nyquist plot and (b) bode plot for mild steel in 0.5 M H_2SO_4 in absence and presence of AMLE.

From the Table 5 and 6, it was evident that the R_t values increased with the increase in the extract concentration. The increase in R_t value could be attributed to the formation of

protective film on metal/solution interface. The protective layer retarded the flow of ions across the metal-acid interface and hence inhibition acknowledged. Further investigation of the results obtained for mild steel in HCl and H_2SO_4 solution revealed that the n values of the inhibited samples was greater than value of n for uninhibited samples. This indicated that the surface heterogeneity decreased in presence of the extract molecules, which occurred due to adsorption of the inhibitor molecules on the most reactive surface sites [Raja et al., 2013]. Also, the values of double layer capacitance (C_{dl}) decreased with increasing AMLE concentration, supporting the increase in corrosion resistance with the inhibitor concentration. The decrease in C_{dl} values could be described according to the following equation [H.H. Hassan, 2006,]-

$$C_{dl} = \frac{\varepsilon\, \varepsilon_o}{d} \qquad (25)$$

where ε is the dielectric constant of the protective layer, ε_o is the permittivity of the free space and d is the thickness of the protective film at the interface.

Table 3.5 Impedance parameters for mild steel in 1.0 M HCl in absence and presence of different concentrations of AM Extract

Conc. (mgL^{-1})	R_s ($\Omega\ cm^2$)	R_t ($\Omega\ cm^2$)	n	Y_o ($10^{-6}\Omega^{-1}cm^{-2}$)	C_{dl} ($\mu F\ cm^{-2}$)	μ_{Rt} (%)
Blank	1.23	30	0.802	147	41.7	-
200	0.95	66	0.809	120	39.0	54.5
300	1.01	84	0.815	100	36.9	64.3
400	0.89	124	0.869	99	33.4	75.8
500	**0.83**	**209**	**0.885**	**83**	**29.1**	**85.7**

Table 3.6 Nyquist plots obtained for mild steel in 0.5 M sulfuric acid with different concentration of inhibitor.

Conc. (mg L^{-1})	R_s (Ω cm^2)	R_t (Ω cm^2)	n	Y_0 ($10^{-6}\Omega^{-1}cm^{-2}$)	C_{dl} (μF cm^{-2})	μ_{Rt} %
Blank	1.25	37	0.808	198	61	-
300	1.32	83	0.810	154	55	56
400	1.28	120	0.815	132	51	70
500	1.70	180	0.820	113	48	80
600	**1.82**	**220**	**0.824**	**89**	**39**	**84**

From the bode plots (Figure 20 b and 21 b) it was evident that phase angle and corrosion impedance increased with the extract concentration. Initially, mild steel corroded at fast rate on immersion in acid media and low phase angle was recorded; however, surface regularity of steel increased in presence of inhibitor and higher phase angle was acknowledged. Figure 22 illustrate accuracy of simulation of the EIS data.

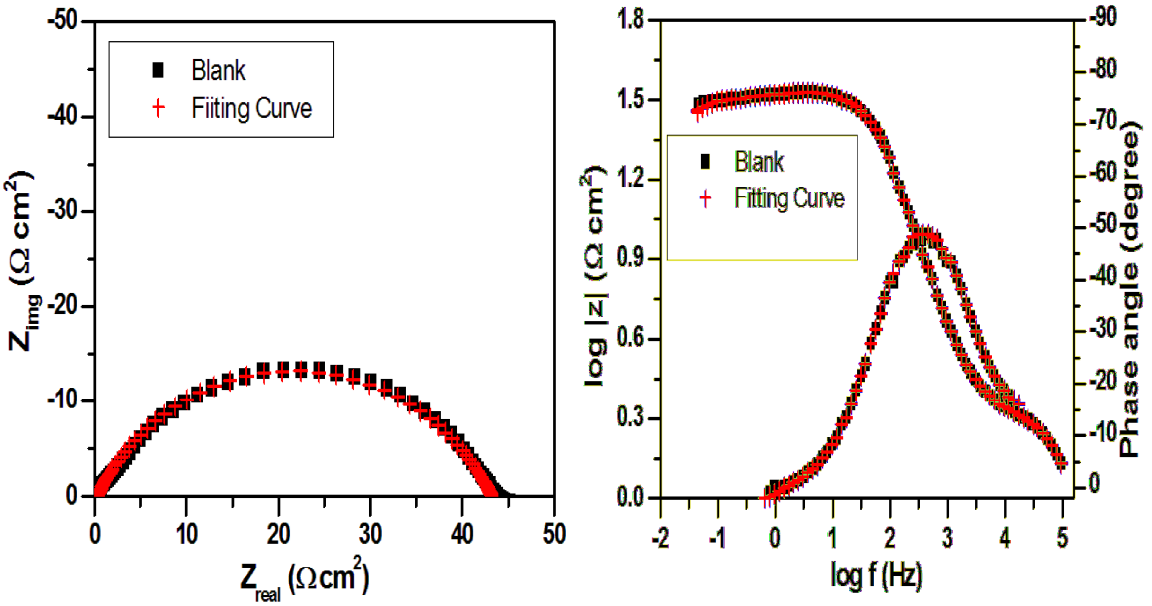

Figure 3.15 Fitting curves showing relation between simulated and experimental data.

The *Argemone Mexicana* extract inhibited the corrosion of mild steel in 1M HCl and 0.5 M H_2SO_4 solutions at all the concentrations used in the study. The inhibition efficiencies (μ_{Rt}) calculated from EIS showed the same trend as those obtained from weight loss and tafel polarization data.

3.5 Surface Morphology Study

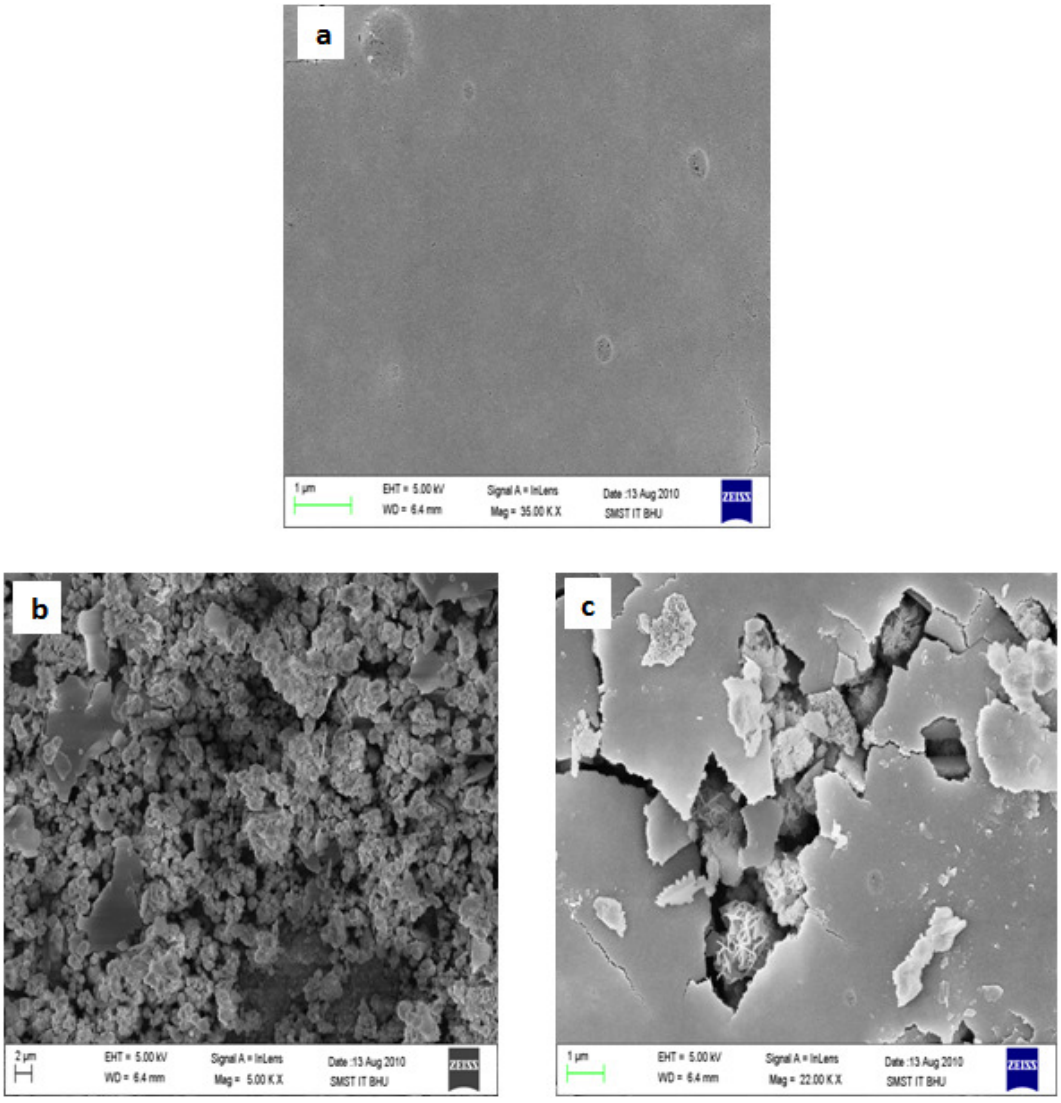

Figure 3.16 SEM images of (a) mild steel (b) corroded steel in HCl and (c) inhibited mild steel.

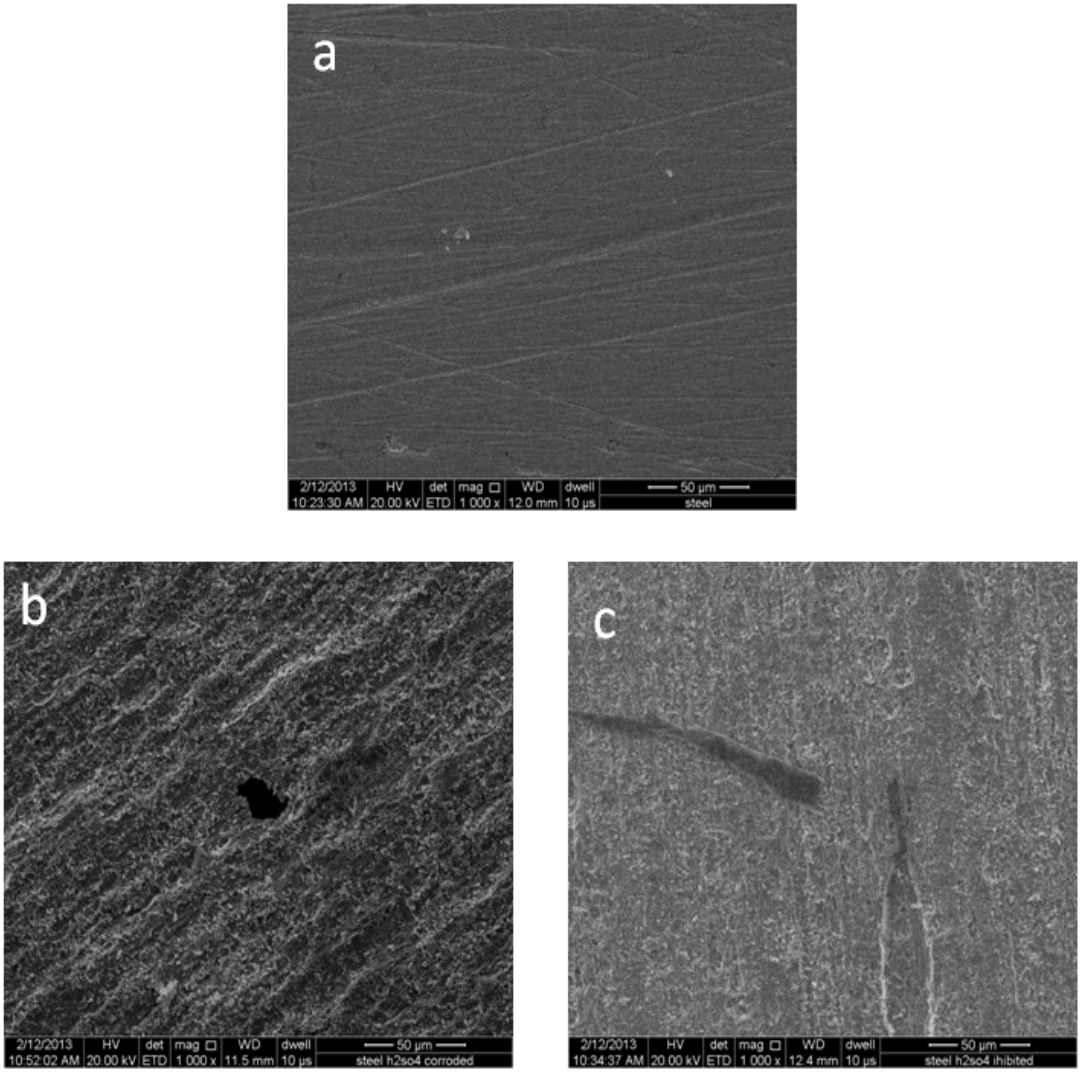

Figure 3.17 SEM images of (a) mild steel (b) corroded steel in H_2SO_4 and (c) inhibited mild steel.

Figure 23 shows the effect of inhibitors on mild steel corrosion in HCl via surface images. Prepared mild steel sample showed a few spots over the surface as shown in Figure 23a. The treatment of test sample with 1M acid caused heavy loss of the surface material, which created many corrosion pits on the metal surface (Figure 23b). However, a significant protection was acknowledged in presence of the extract (500 mg L^{-1}). From Figure 23c it is evident that mild steel was protected by corrosion attack via an inhibitive

layer of the extract molecules. But, some cracks could be observed on the surface that occurred due to aggressive acid attack.

Figure 24 illustrates surface morphology of steel, uninhibited steel and inhibited steel in H_2SO_4. It is evident from Figure 24a that test sample was having smooth surface. However, some surface scratches could be clearly seen, which occurred due to uneven polishing of the samples during preparation. When mild steel was immersed in sulfuric acid, an intense corrosion reaction took place and made the entire surface highly rough and irregular (Figure 24b). A small hole could be seen on the middle of the test sample, showing intensity of the acid attack. On the other side, drastic change in surface morphology of mild steel was acknowledged in comparison to the surface morphology of corroded sample (24c).

3 D AFM images of the mild steel sample in HCl and H_2SO_4 solutions in absence and presence of inhibitor are shown in Figure 25. The roughness of the prepared mild steel specimen was measured as 15 nm, which was drastically increased due to aggressive attack of HCl (90 nm) and H_2SO_4 (115 nm), as shown in Figure 25 a-c. In contrast, significant changes occurred in presence of the extracts, and roughness of the test samples decreased to 42 nm (inhibited in HCl) and 65 nm (inhibited in H_2SO_4). These facts showed good agreement of the results with the results obtained by SEM technique.

As a summary of the surface morphology study, it could be concluded that Argemone Mexicana extract successfully retarded corrosion of mild steel in both acid media. However, the extract was more efficient in hydrochloric acid than sulfuric acid.

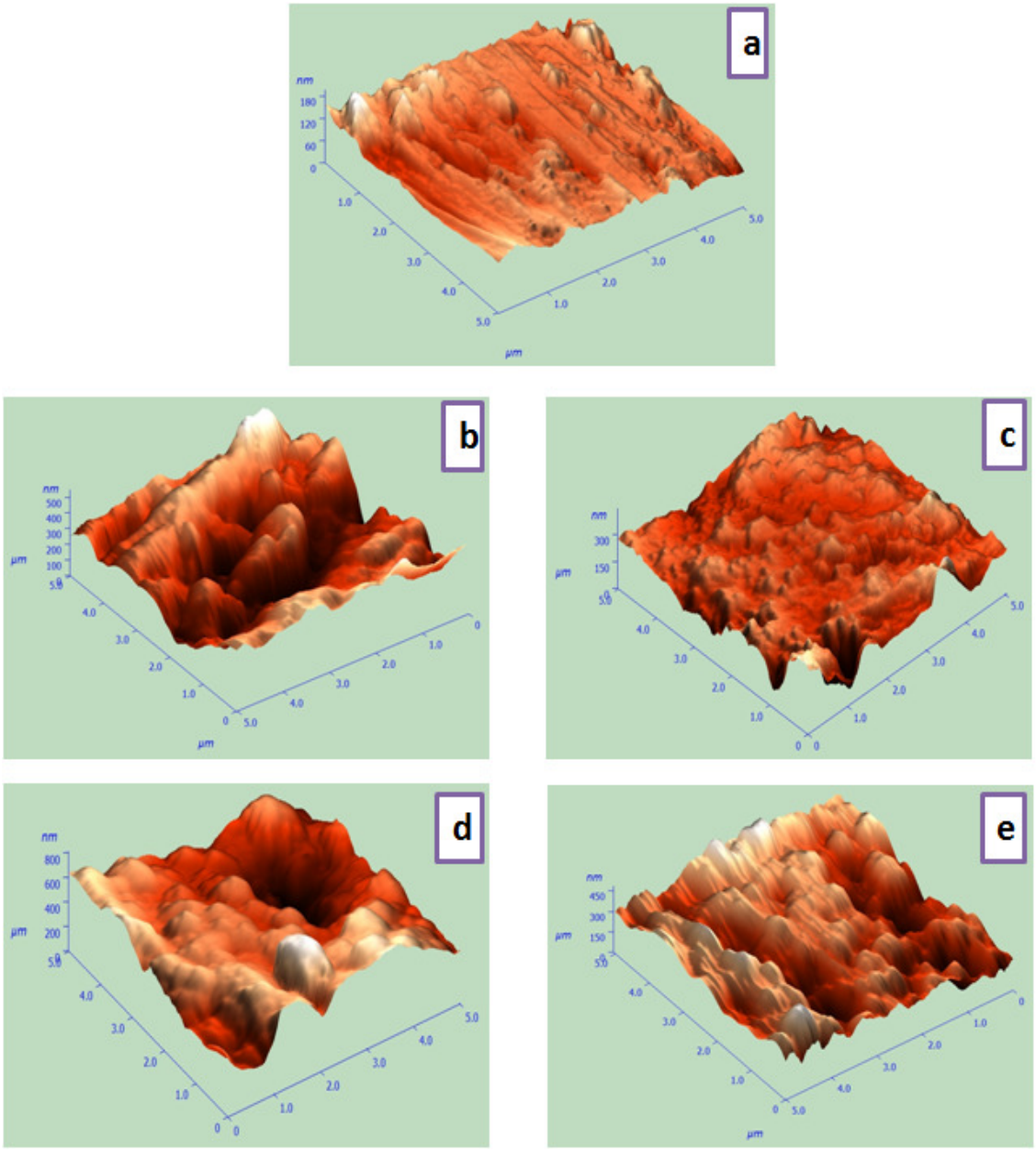

Figure 3.18 3D AFM images of (a) mild steel, (b) HCl corroded steel, (c) inhibited steel, (d) H2SO4 corroded surface and (e) inhibited steel in sulfuric acid.

3.6 Mechanism of Corrosion Inhibition

Argemone Mexicana plant is a rich source of various compounds [Dash et al, 2011]. Among them, some moieties are toxic in nature; however, aqueous extract of plant leaves

do not have alkaloids and hence show no toxicity. AMLE contain several bioactive compounds (HPLC study). These organic moieties are rich in the functional groups that have nitrogen and oxygen as well as aromatic rings in their structure (FT-IR). The organic compounds of the extract, such as, Saponins, Tannins, Flavoniods and amino acids (Figure 26) may exist in the acidic solution either in protonated form or neutral form. Accordingly, molecular adsorption of inhibitor can take place via electrostatic forces (physical adsorption) or chemical boding (chemisorption).

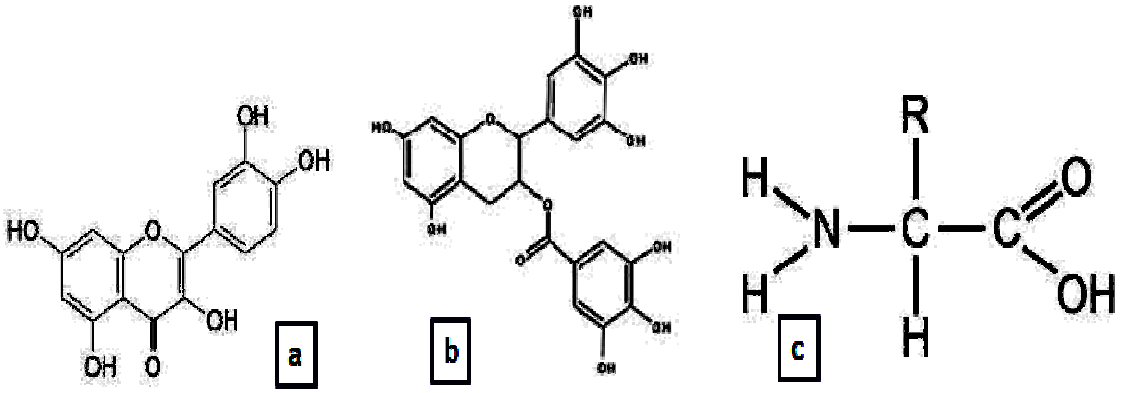

Figure 3.19 Chemical structures of (a) Flavonoids, (b) Tannins and (c) amino acids

Through inspection of the chemical structures of the key chemical constituents of AMLE, it could be stated that they might be protonized in acidic media. However, it was still difficult for inhibitor molecules to interact with positively charged mild steel. In this case, it was possible that acid anions, Cl^- and SO_4^{2-}, adsorbed on the steel surface and triggered the physical bond formation between metal and AMLE. Along with the electrostatic interactions, the extract molecules (π electrons of aromatic rings) could form a covalent bond with d-orbital electrons of iron [Deng and Li, 2012, Herrag et al., 2010]. This fact was also supported by positive and increasing Ea and ΔG^0 values. Additionally, lone pair electrons of AMLE (from hetroatoms O, N) might react with ionized iron molecules and

produce iron-inhibitor complexes. Eventually, these complex compounds could form of an inhibitive layer at steel/acid interface and retard the corrosion of mild steel in acid media.